www.czasopisma.pan.pl PAN POLSKA AKADEMIA NAUK www.journals.pan.pl

jet INTL JOURNAL OF ELECTRONICS AND TELECOMMUNICATIONS, 2017, VOL. 63, NO. 3, PP. 255-260
Manuscript received June 4, 2016; revised June, 2017. DOI: 10.1515/eletel-2017-0034

Analysis of Substrate Integrated Waveguide (SIW) Resonator and Design of Miniaturized SIW Bandpass Filter

Ahmed Rhbanou, Seddik Bri, and Mohamed Sabbane

***Abstract*—In this paper, the substrate integrated waveguide (SIW) resonator is designed to study the influence of dielectric materials on its operating parameters (insertion loss, fractional bandwidth and unloaded *Q*-factor). The results obtained show that the use of high permittivity substrate in the SIW resonator by increasing its thickness allows reducing the size of resonator by causing the increase in its unloaded *Q*-factor. A SIW bandpass filter is designed using low temperature co-fired ceramic (LTCC) technology and high permittivity substrate. The filter has a fractional bandwidth of 27 % centered at 14.32 GHz with insertion loss of 0.7 dB.**

***Keywords*—substrate integrated waveguide, dielectric materials, cavity resonator, band-pass filter, low temperature co-fired ceramic**

I. Introduction

MICROWAVE filters are widely used in the wireless communication systems, especially communication satellites. Rectangular waveguide filters are characterized by the high *Q*-factor and the low losses. However, their fabrications are very expensive and their interactions with planar structures are very difficult. In order to overcome these problems, a new technology has been proposed in the realization of the millimeter-wave filters, called the substrate integrated waveguide (SIW). The SIW is composed of two solid conductor planes separated by a dielectric substrate with two arrays of via holes in the both side walls. The SIW filters take the advantages of easy integration, high *Q*-factor, low cost and low losses [1]. On the other, LTCC (Low Temperature Co-fired Ceramic) is a multilayer ceramic technology which allows producing multilayer hybrid integrated circuits. This technology is extremely useful for RF and microwave applications, due to its merits of low material costs and good thermal conductivity [2]. In this paper, the SIW resonator is analyzed to study the influence of dielectric materials. A SIW bandpass filter is designed using LTCC technology and high permittivity substrate. The structures are designed and simulated by using Ansoft HFSS.

II. Design of SIW Cavity

The essential parameters of the SIW cavity are the distance between the holes (*P*), the diameter of the metallic via (*D*), the length (L_{SIW}) and the width (W_{SIW}). Thus, the propagation properties in the SIW cavity is very similar in a rectangular waveguide cavity filled with the same dielectric (ε_r) with width (W_{eff}) and length (L_{eff}) as shown in Fig. 1.

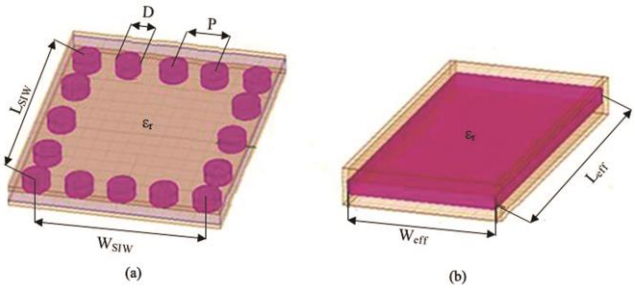

Fig. 1. (a) SIW cavity, (b) conventional rectangular waveguide cavity.

The width and the length of the SIW cavity are determined from Eqs. (1), (2) and (3), with $P < 4\,D$ and $P < \lambda_0\,(\varepsilon_r/2)^{1/2}$ and λ_0 is the space wavelength [3]-[11].

$$W_{eff} = W_{SIW} - \frac{D^2}{0.95P} \tag{1}$$

$$L_{eff} = L_{SIW} - \frac{D^2}{0.95P} \tag{2}$$

$$f_r(TE_{m0p}) = \frac{c}{2\sqrt{\varepsilon_r}}\sqrt{\left(\frac{m}{W_{eff}}\right)^2 + \left(\frac{p}{L_{eff}}\right)^2} \tag{3}$$

The unloaded *Q*-factor is defined as [12], [13]:

$$Q = \left(\frac{1}{Q_d} + \frac{1}{Q_c}\right)^{-1} \tag{4}$$

where Q_c depends only on the ohmic losses in the waveguide walls and is given by (5) [13].

$$Q_c = \frac{(KW_{eff}L_{eff})^3 h\eta}{2\pi^2 R_S\left(2h(W_{eff})^3 + 2h(L_{eff})^3 + L_{eff}(W_{eff})^3 + W_{eff}(L_{eff})^3\right)} \tag{5}$$

and Q_d depends only on losses in the dielectric and is given by (6) [13].

$$Q_d = \frac{1}{\tan\delta} \tag{6}$$

With:

$$R_S = \sqrt{\frac{\omega\mu_0}{2\sigma}};\quad \eta = \frac{377}{\sqrt{\varepsilon_r}};\quad K = \frac{2\pi f_r(TE_{101})\sqrt{\varepsilon_r}}{c} \tag{7}$$

A. Rhbanou and M. Sabbane are with Department of Mathematics, FSM, Moulay Ismail University, Meknes, 50000, Morocco (e-mails: rhbanou@gmail.com; m.sabbane@umi.ac.ma).

S. Bri is with Material and Instrumentations group (MIN), Electrical Engineering Department, ESTM, Moulay Ismail University, Meknes, 50000, Morocco (e-mail: briseddik@gmail.com).

where K is the wave number in the resonator, $tan\delta$ is the loss tangent of the dielectric, R_s is the surface resistance of the cavity ground planes and η is the intrinsic impedance.

From these expressions, Figure 2 shows the evolution of unloaded Q-factor of the square waveguide cavity filled with dielectric ($W_{eff} = L_{eff}$) resonating at 9.13 GHz in the TE_{101} mode as a function of its thickness by varying its dielectric material. The silver metal walls (σ = 6.1 107 S/m) are used for the metallization.

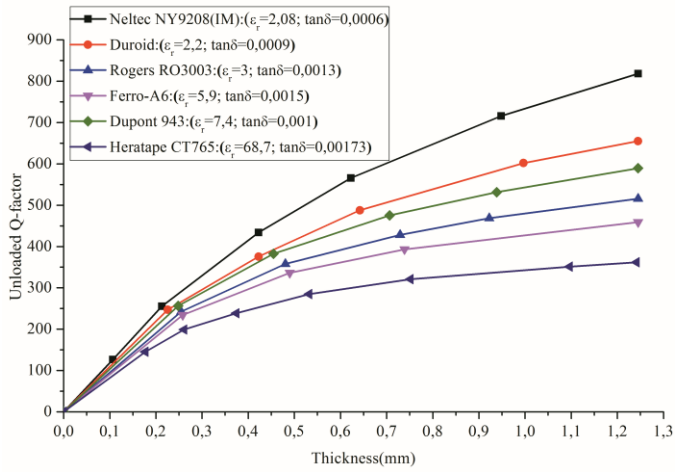

Fig. 2. Evolution of unloaded Q-factor of the square waveguide cavity filled with dielectric ($W_{eff} = L_{eff}$) resonating at 9.13 GHz in the TE_{101} mode as a function of its thickness by varying its dielectric material.

Figure 2 shows that the increase of the thickness of each dielectric material used in square waveguide cavity filled with dielectric ($W_{eff} = L_{eff}$) resonating at 9.13 GHz in the TE_{101} mode has caused an increase the unloaded Q-factor of cavity. Thus, the use of substrates with low dielectric loss allows obtaining very interesting results for high frequency applications.

III. Analysis of SIW Resonator

The TE_{101}-mode-based SIW resonator is presented by a square SIW cavity ($W_{SIW} = L_{SIW}$) and tapered transitions with D = 0.15 mm and P = 0.375 mm. Figure 3 shows geometry parameters of SIW resonator.

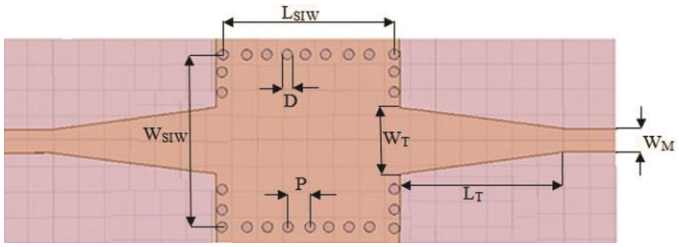

Fig. 3. Square SIW cavity with tapered transitions.

The SIW resonator resonating at 9.13 GHz in the TE_{101} mode is simulated by varying its dielectric material and its thickness, to provide estimates of its fractional bandwidth, its insertion loss and its unloaded Q-factor. The physical parameters of SIW resonator for several dielectric materials as a function of its thickness are shown in Table I.

As illustrated in Table I, the use of high permittivity substrate in the SIW resonator allows reducing the size of resonator.

The evolution the fractional bandwidth, the insertion loss and the unloaded Q-factor of the SIW resonator resonating at 9.13 GHz in the TE_{101} mode as a function of its thickness by varying its dielectric material are shown in Fig. 4.

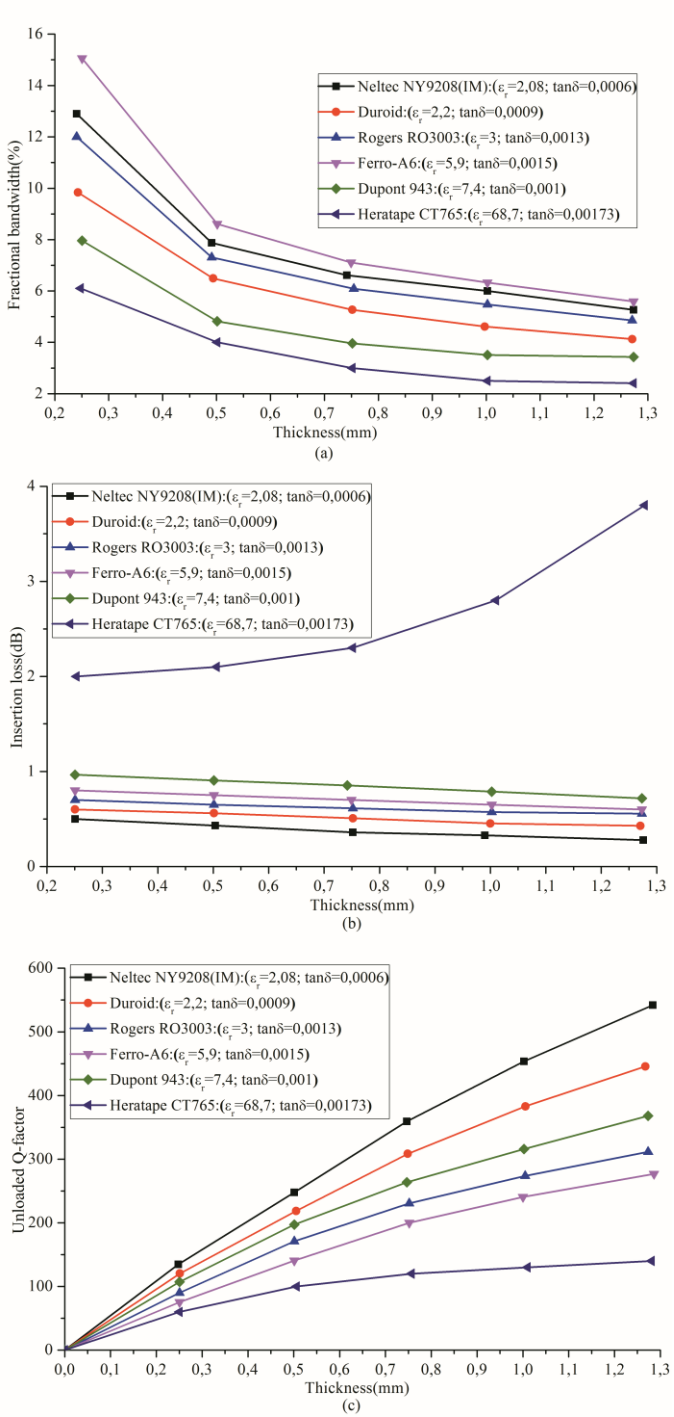

Fig. 4. (a) Evolution the fractional bandwidth of the SIW resonator resonating at 9.13 GHz in the TE_{101} mode as a function of its thickness by varying its dielectric material, (b) evolution the insertion loss of the SIW resonator resonating at 9.13 GHz in the TE_{101} mode as a function of its thickness by varying its dielectric material, (c) evolution the unloaded Q-factor of the SIW resonator resonating at 9.13 GHz in the TE_{101} mode as a function of its thickness by varying its dielectric material.

TABLE I
PHYSICAL DIMENSIONS OF SIW RESONATOR FOR DIFFERENT DIELECTRIC MATERIALS AS A FUNCTION OF ITS THICKNESS

Dielectric materials	Thickness of the SIW resonator (mm)	$W_{SIW}=L_{SIW}$ (mm)	L_T (mm)	W_T (mm)	WM (mm)
Neltec NY9208(IM) ε_r=2.08 tanδ=0.0006	0.25	14.82	16.38	5.868	0.79
	0.50	14.92		5.908	1.59
	0.75	14.96		5.924	2.39
	1.00	14.98		5.932	3.19
	1.27	15.00		5.940	4.05
Duroid ε_r=2.2 tanδ=0.0009	0.25	14.48	16.00	5.732	0.77
	0.50	14.56		5.764	1.54
	0.75	14.60		5.78	2.31
	1.00	14.62		5.788	3.08
	1.27	14.64		5.796	3.91
Rogers RO3003 ε_r=3 tanδ=0.0013	0.25	12.34	14.08	4.876	0.62
	0.50	12.42		4.908	1.25
	0.75	12.44		4.916	1.88
	1.00	12.46		4.924	2.50
	1.27	12.48		4.932	3.18
Ferro-A6 ε_r=5.6 tanδ=0.0015	0.25	8.78	10.57	3.452	0.38
	0.50	8.82		3.468	0.76
	0.75	8.83		3.472	1.14
	1.00	8.84		3.474	1.53
	1.27	8.84		3.476	1.94
Dupont 943 ε_r=7.4 tanδ=0.001	0.25	7.98	9.60	3.132	0.31
	0.50	8.00		3.140	0.62
	0.75	8.02		3.152	0.93
	1.00	8.03		3.156	1.25
	1.27	8.04		3.156	1.58
Heratape CT765 ε_r=68.7 tanδ=0.00173	0.25	2.70	3.53	1.020	0.10
	0.50	2.71		1.024	0.20
	0.75	2.72		1.208	0.30
	1.00	2.73		1.033	0.40
	1.27	2.73		1.034	0.50

As illustrated in Fig. 4, the increase of the thickness of each dielectric material used in the SIW resonator has caused an increase the unloaded *Q*-factor and the reduction the fractional bandwidth of resonator. Thus, the use of a dielectric material that has a high permittivity in the SIW resonator has caused an increasing the insertion losses of resonator.

IV. FILTER DESIGN AND ANALYSIS

A second-order bandpass filter is designed to meet the following specifications, a center frequency is f_0 = 14.32 GHz and a fractional bandwidth is *FBW* = 27 %. The return loss is better than 20 dB and the rejection ≥ 10 dB for frequencies ≥ 27 GHz. The coupling routing diagram of the proposed filter is shown in Fig. 5, where each line shows a direct coupling and each node represents a resonator.

Applying the classical Chebyshev synthesis, the element values of the lowpass prototype filter are g_0 = 1, g_1 = 0.4489, g_2 = 0.4078, g_3 = 1.1008 [14]. The external quality factors of the filter at the input (Q_{ein}) and output (Q_{eout}) can be synthesized by formula (8) shown as follows [14].

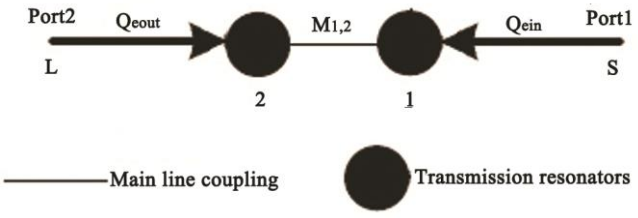

Fig. 5. Coupling and routing diagram of the proposed second-order bandpass filter.

$$Q_{ein} = Q_{eout} = \frac{g_0 g_1}{FBW} = 1.66 \tag{8}$$

The coupling coefficient ($M_{1,2}$) is given by (9) [14]:

$$M_{1,2} = \frac{FBW}{\sqrt{g_1 g_2}} = 0.63 \tag{9}$$

The coupling matrix [***M***] of the proposed filter is given by formula (10).

$$[M]=\begin{bmatrix} 0 & 0.63 \\ 0.63 & 0 \end{bmatrix} \quad (10)$$

The filter is composed of two SIW resonators. Figure 6 shows the top view of the proposed filter. The iris is used to form the inter-resonator coupling structure ($M_{1,2}$), the input and output are coupled through coplanar waveguide (CPW).

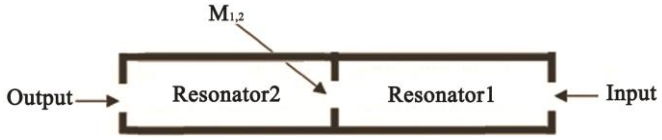

Fig. 6. Top view of the proposed second-order SIW bandpass filter.

The substrate of the filter is made of six 0.084 mm thick layers of Heratape CT765 (ε_r =68.7 and $tan\delta$ = 0.00173). The resonant frequency of TE_{101} mode in each cavity of filter is about 14.32 GHz.

The external quality factor (Q_e) for resonator 1 and 2 is calculated by using the model shown in Fig. 7, a SIW cavity with a circular hole etched on top metal layer and a coplanar waveguide (CPW) with the following conditions: W_{SIW} = L_{SIW} = 2.64 mm, D = 0.15 mm, P = 0.375 mm, L_M = 0.78 mm, W_M = 0.2268 mm, R = 0.97 mm, L_1 = 3.6 mm, W = 3.24 mm, n = 0.1 mm, a = 1.32 mm, b = 0.35 mm and *slot height* = 0.2 mm.

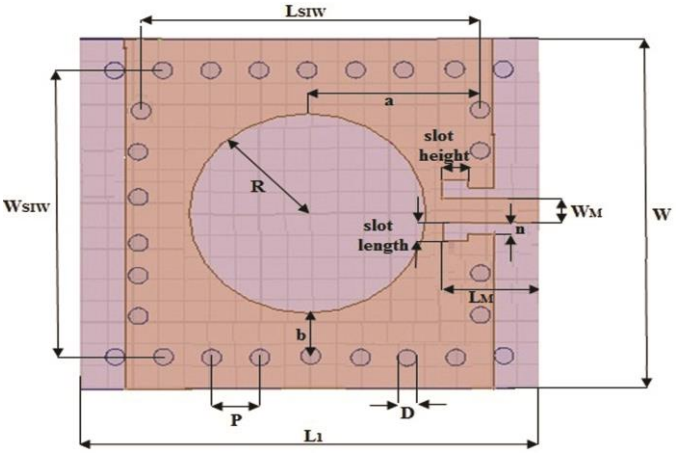

Fig. 7. Geometry of the proposed model to calculate the external quality factor (Q_e) for resonator 1 and 2, where W_{SIW} = L_{SIW} = 2.64 mm, D = 0.15 mm, P = 0.375 mm, L_M = 0.78 mm, W_M = 0.2268 mm, R = 0.97 mm, L_1 = 3.6 mm, W = 3.24 mm, n = 0.1 mm, a = 1.32 mm, b = 0.35 mm and *slot height* = 0.2 mm.

The external quality factor (Q_e) is controlled by changing the *slot length* of the conventional coplanar waveguide (CPW). Q_e is obtained from the simulation by using this formula [15]:

$$Q_e = \frac{f_0}{\Delta f} \quad (11)$$

Where f_0 is the resonant frequency of the resonator (SIW resonator 1 or 2) and Δf is the 3-dB bandwidth centre at the resonant frequency.

Figure 8 shows the evolution of the external quality factor (Q_e) as a function of *slot length* of CPW, where W_{SIW} = L_{SIW} = 2.64 mm, D = 0.15 mm, P = 0.375 mm, L_M = 0.78 mm, W_M = 0.2268 mm, R = 0.97 mm, L_1 = 3.6 mm, W = 3.24 mm, n = 0.1 mm, a = 1.32 mm, b = 0.35 mm and *slot height* = 0.2 mm, obtained using Ansoft HFSS.

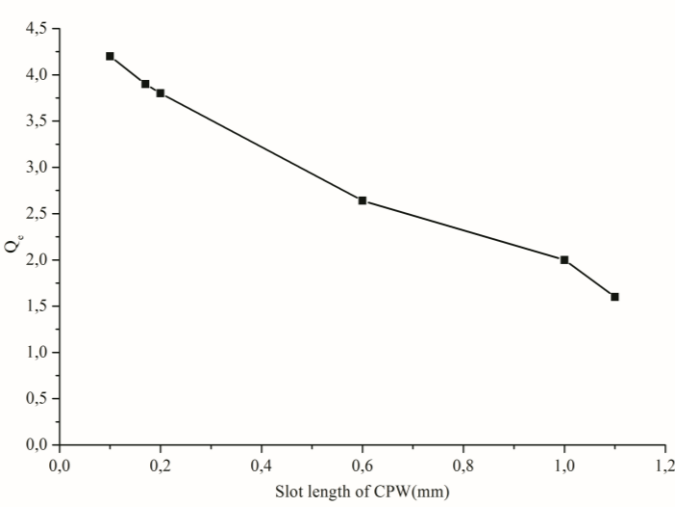

Fig. 8. External quality factor (Q_e) evaluated as a function of *slot length* of CPW, where W_{SIW} = L_{SIW} = 2.64 mm, D = 0.15 mm, P = 0.375 mm, L_M = 0.78 mm, W_M = 0.2268 mm, R = 0.97 mm, L_1 = 3.6 mm, W = 3.24 mm, n = 0.1 mm, a = 1.32 mm, b = 0.35 mm and *slot height* = 0.2 mm.

As illustrated in Fig. 8, when the slot length of CPW increases the external quality factor (Q_e) is decreasing. Thus, as required for the filter specification, Q_e = 1.66 is obtained at *slot length* of CPW = 1.05 mm.

The coupling between the two SIW resonators is performed by an *iris opening*. This structure is shown in Fig. 9, with the following conditions: W_{SIW} = L_{SIW} = 2.64 mm, D = 0.15 mm, P = 0.375 mm, R = 0.97 mm, L = 6.24 mm, W = 3.24 mm, a = 1.32 mm and b = 0.35 mm.

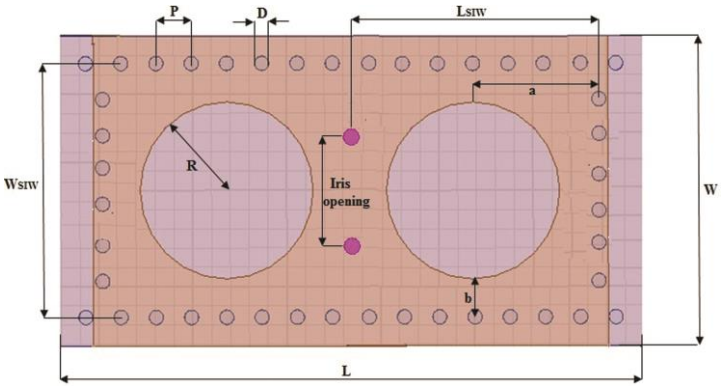

Fig. 9. Geometrical parameters of the coupling between the two SIW resonators, where W_{SIW} = L_{SIW} = 2.64 mm, D = 0.15 mm, P = 0.375 mm, R = 0.97 mm, L = 6.24 mm, W = 3.24 mm, a = 1.32 mm and b = 0.35 mm.

The coupling coefficient (M) is defined as [15]:

$$M = \pm \frac{f_e^{\,2} - f_m^{\,2}}{f_e^{\,2} + f_m^{\,2}} \quad (12)$$

Where M is the coupling coefficient between two SIW resonators, f_e is the higher resonant frequency and f_m is the lower resonant frequency.

Figure 10 shows the evolution of the coupling coefficient (M) as a function of the *iris opening*, where W_{SIW} = L_{SIW} = 2.64 mm, D = 0.15 mm, P = 0.375 mm, R = 0.97 mm, L = 6.24 mm, W = 3.24 mm, a = 1.32 mm and b = 0.35 mm, obtained using Ansoft HFSS.

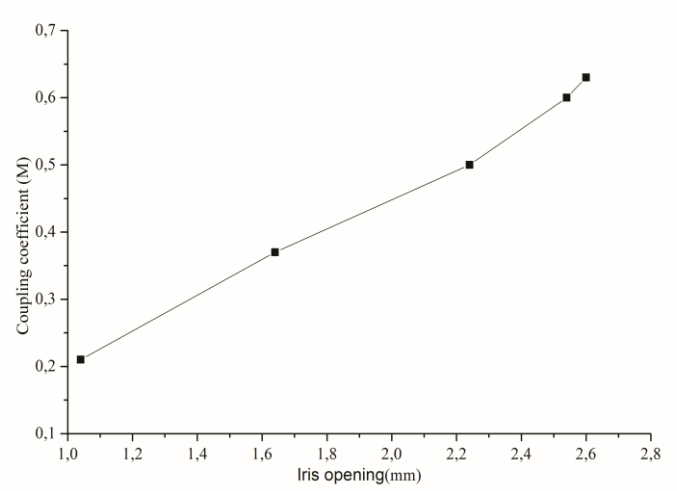

Fig. 10. Coupling coefficient (*M*) evaluated as a function of the *iris opening*, where $W_{SIW} = L_{SIW} = 2.64$ mm, $D = 0.15$ mm, $P = 0.375$ mm, $R = 0.97$ mm, $L = 6.24$ mm, $W = 3.24$ mm, $a = 1.32$ mm and $b = 0.35$ mm.

According to Fig. 10, when the iris opening increases the coupling coefficient (*M*) becomes large, as required for the filter specification, the coupling coefficients $M_{1,2} = 0.63$ can be obtained for a *iris opening* = 2.6 mm.

TABLE II
PHYSICAL DIMENSIONS OF SECOND-ORDER SIW BANDPASS FILTER IN LTCC TECHNOLOGY USING HIGH PERMITTIVITY SUBSTRATE

Symbol	Dimension (mm)	Symbol	Dimension (mm)
D	0.15	d	0.425
P	0.375	Iris opening	1.04
L_{SIW}	2.64	Slot length of CPW	0.17
W_{SIW}	2.64	Slot height of CPW	0.2
R	0.92	Substrate thickness	0.504
W_M	0.2268	L_M	0.78
W	3.24	a	1.32
L	6.24	b	0.4
n	0.1		

Figure 11 shows the geometrical parameters of second-order SIW bandpass filter in LTCC technology using high permittivity substrate.

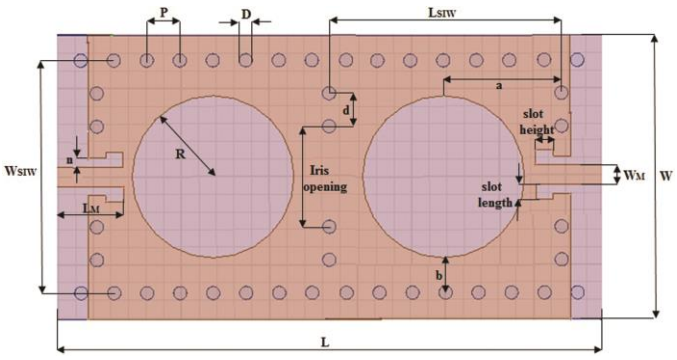

Fig. 11. Top view of second-order SIW bandpass filter in LTCC technology using high permittivity substrate.

After optimization by Ansoft HFSS, the optimal parameters of the filter (Fig. 11) are provided in Table II.

The simulation results for S-parameters of second-order SIW bandpass filter in LTCC technology using high permittivity substrate are shown in Fig. 12.

TABLE III
COMPARISON BETWEEN THE PROPOSED FILTER AND THE FILTERS PRESENTED IN REFERENCES

Reference filter	Central frequency (GHz)	Fractional bandwidth (%)	Insertion loss (dB)	Return loss (dB)	Size (mm^3)
[16]	10.05	3	3.16	>20	46.2×28.6×5.68
[17]	35.8	2.79	4.2	>14	9.5×3.1×1.3
[18]	8	11.87	1.2	>10	9.6×9.6×1.4
[19]	35	10	0.65	>20	9×3×0.297
Proposed	14.32	27	0.7	>20	6.24×3.24×0.504

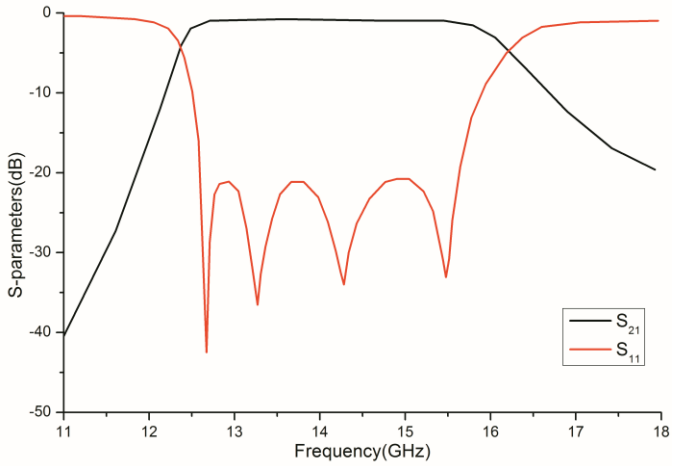

Fig. 12. Simulated S-parameters of second-order SIW bandpass filter in LTCC technology using high permittivity substrate.

Simulated results presented in Fig. 12 show that the filter has a fractional bandwidth of 27 % centered at 14.32 GHz with insertion loss of 0.7 dB and return loss of 21 dB. The size of this filter is only $6.24 \times 3.24 \times 0.504$ mm^3.

In order to verify the properties of proposed filter, a comparison between the proposed filter and the filters reported in the references are presented in Table III.

In According to the comparisons (Table III), the filters in [16], [17] have the return losses quite good, but their insertion losses are much higher than that of the proposed one. Although the filter in [18] has a low insertion loss, their return loss is not good enough. Thus, the filter in [19] has good performance on the whole, but their fractional bandwidth is extremely small than that of the proposed filter.

Generally, the proposed filter proves low insertion loss, better return loss and small dimensions.

V. CONCLUSION

In this paper, a detailed analysis was done on SIW resonator. The results obtained show that the use of high permittivity substrate in the SIW resonator allows reducing the size and the increase the insertion losses of resonator. Thus, the increase of the thickness of each dielectric material used in the SIW resonator has caused the increase the unloaded *Q*-factor and the reduction the fractional bandwidth of the resonator.

The wideband SIW bandpass filter in LTCC technology using high permittivity substrate has been designed, by proving low insertion loss, better return loss and small dimensions. The filter has a fractional bandwidth of 27 % centered at 14.32 GHz with insertion loss of 0.7 dB and return loss of 20 dB. The size of this filter is only $6.24 \times 3.24 \times 0.504$ mm^3.

The proposed filter has small size and low loss, can be directly integrated with other circuits without any additional mechanical assembling tuning, this filter is useful for microwave and millimeter-wave applications.

REFERENCES

[1] Y. Cassivi, L. Perregrini, P. Arcioni, M. Bressan, K. Wu, and G. Conciauro, "Dispersion Characteristics of Substrate Integrated Rectangular Waveguide," *IEEE Microwave and Wireless Components Letters*, vol. 12, pp. 333–335, Sept. 2002.

[2] J. H. Lee, S. Pinel, J. Papapolymerou, J. Laskar, and M. M. Tentzeris, "Low-Loss LTCC Cavity Filters Using System-on-Package Technology at 60 GHz," *IEEE Transactions on Microwave Theory and Techniques*, vol. 53, pp. 3817–3824, Dec. 2005.

[3] D. Deslandes and K. Wu, "Accurate modeling, wave mechanism, and design consideration of a substrate integrated waveguide," *IEEE Transactions on Microwave Theory and Techniques*, vol. 54, pp. 2516–2526, Jun. 2006.

[4] A. Rhbanou, S. Bri, and M. Sabbane, "Design of Substrate Integrated Waveguide Band Pass Filter Based on CSRR-EBG," *International Journal of Microwave and Optical Technology*, vol. 11, pp. 7–14, Jan. 2016.

[5] T. Djerafi and K. Wu, "Super-Compact Substrate Integrated Waveguide Cruciform Directional Coupler," *IEEE Microwave and Wireless Components Letters*, vol. 17, pp. 757–759, Nov. 2007.

[6] X.-C. Zhang, Z.-Y. Yu, and J. Xu, "Novel Band-Pass Substrate Integrated Waveguide (SIW) Filter Based on Complementary Split Ring Resonators (CSRRS)," *Progress in Electromagnetics Research*, vol. 72, pp. 39–46, 2007.

[7] F. Xu and K. Wu, "Guided-Wave and Leakage Characteristics of Substrate Integrated Waveguide," *IEEE Transactions on Microwave Theory and Techniques*, vol. 53, pp. 66–73, Jan. 2005.

[8] A. Rhbanou, S. Bri, and M. Sabbane, "Design of Dual-Mode Substrate Integrated Waveguide Band-Pass Filters," *Circuits and Systems*, vol. 6, pp. 257–267, Dec. 2015.

[9] Y. Huang, Z. Shao, and L. Liu, "A Substrate Integrated Waveguide Bandpass Filter Using Novel Defected Ground Structure Shape," *Progress in Electromagnetics Research*, vol. 135, pp. 201–213, 2013.

[10] Y. Arfat, S. P. Singh, S. Arya, and S. Khan, "Modelling, Design and Parametric Considerations for Different Dielectric Materials on Substrate Integrated Waveguide," *Wseas Transactions on Communications*, vol. 13, pp. 94–98, 2014.

[11] A. Rhbanou, S. Bri, and M. Sabbane, "Design of X-Band Substrate Integrated Waveguide Bandpass Filter with Dual High Rejection," *Microwave and Optical Technology Letters*, vol. 57, pp. 1744–1752, Jul. 2015.

[12] A. Rhbanou, S. Bri, and M. Sabbane, "Design of K-Band Substrate Integrated Waveguide Band-Pass Filter with High Rejection," *Journal of Microwaves, Optoelectronics and Electromagnetic Applications*, vol. 14, pp. 155–169, Dec. 2015.

[13] D. M. Pozar, "Microwave Engineering," Hoboken: Wiley, 2012.

[14] J. S. Hong and M. J. Lancaster, "Microstrip Filters for RF/Microwave Applications," Chichester: Wiley, 2001.

[15] T.-M. Shen, C.-F. Chen, T.-Y. Huang, and R.-B. Wu, "Design of Vertically Stacked Waveguide Filters in LTCC," *IEEE Transactions on Microwave Theory and Techniques*, vol. 55, pp. 1771–1779, Aug. 2007.

[16] A. Ismail, M. S. Razalli, M. A. Mahdi, R. S. A. R. Abdullah, N. K. Noordin, and M. F. A. Rasid, "X-band Trisection Substrate-Integrated Waveguide Quasi-Elliptic Filter," *Progress in Electromagnetics Research*, vol. 85, pp. 133–145, 2008.

[17] Z. Wang, S. Bu, and Z. Luo, "A KA-Band Third-Order Cross-Coupled Substrate Integrated Waveguide Bandpass Filter Base on 3D LTCC," *Progress in Electromagnetics Research C*, vol. 17, pp. 173–180, 2010.

[18] Z. Xiangjun, M. Caoyuan, and C. Deqiang, "Compact Dual-Passband LTCC Filter Exploiting Eighth-Mode SIW and SIW Hybrid with Coplanar Waveguide," *Electronics Letters*, vol. 50, pp. 1849–1851, Nov. 2014.

[19] B. Liu, J. Zhou, R. Liu, Q. Wu, K. Zhang, "A 35 GHz Reduced-Size Bandpass Filter Based on SIW in LTCC Technology," in *Proc. of IEEE International Conference on Microwave Technology and Computational Electromagnetics*, China, 2013, pp. 77–80.